Radio emission from pulsar-planet magnetospheric interaction

Miljenko Čemeljić

Institute of Physics, Silesian University in Opava, Czech Republic

&

Nicolaus Copernicus Astronomical Center, PAN Warsaw

&

ASIAA Visiting Scholar, Taipei, Taiwan

SILESIAN UNIVERSITY
INSTITUTE OF PHYSICS IN OPAVA

PAN
POLSKA AKADEMIA NAUK

Centrum Astronomiczne im. Mikołaja Kopernika
Polskiej Akademii Nauk

ASIAA

in collaboration with Jacobo Varela, Universidad Carlos III de Madrid,

Maurizio Falanga, ISSI and Bern University
and

Ruchi Mishra in CAMK, Warsaw

Outline

- Introduction, aurora in Solar System
- Numerical simulations of star-planet magnetosphere interaction
- Results for aurora on planets around Sun and exoplanets
- Planets around pulsars, list of (possible) objects
- Preliminary results in our simulations with pulsar parameters
- Summary

Introduction-Earth aurora

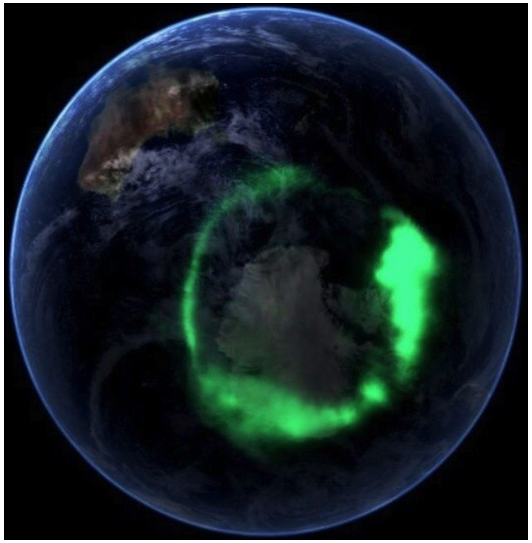

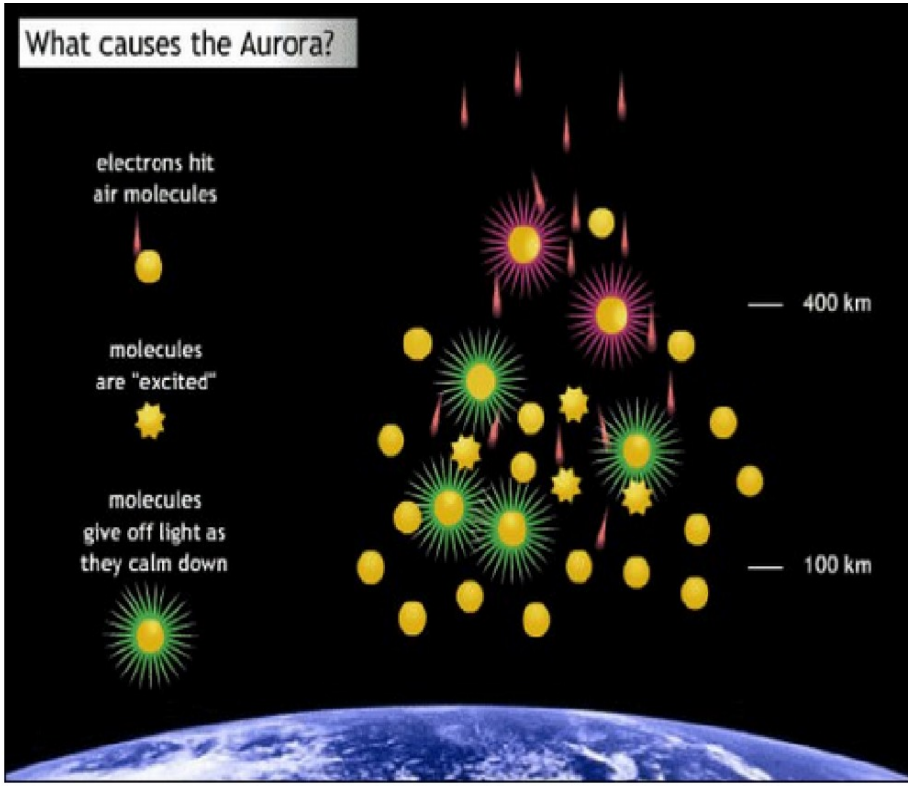

High-speed particles from the Sun, mostly electrons, strike oxygen and nitrogen atoms in Earth's upper atmosphere. Credit: NASA

Aurora, named **aurora borealis** (by the Greek goddess of dawn, Aurora, and Greek name for northern wind, Boreas) by Pierre Gassendi in 1621, forms as an outcome of the interaction of a parent star magnetic field with the planetary field. On Earth, aurora is visible close to the geographic poles, since they are also currently close to the magnetic poles of Earth.

Different gases in the upper layers of the atmosphere are emitting light of different colors in collision with particles from the solar wind (mostly electrons in this case). Oxygen emits greenish or brown-red, and nitrogen blue or red light.

Aurora on Mercury, Venus

Except on Earth, auroras are found on most of the planets in the Solar system.

Mercury

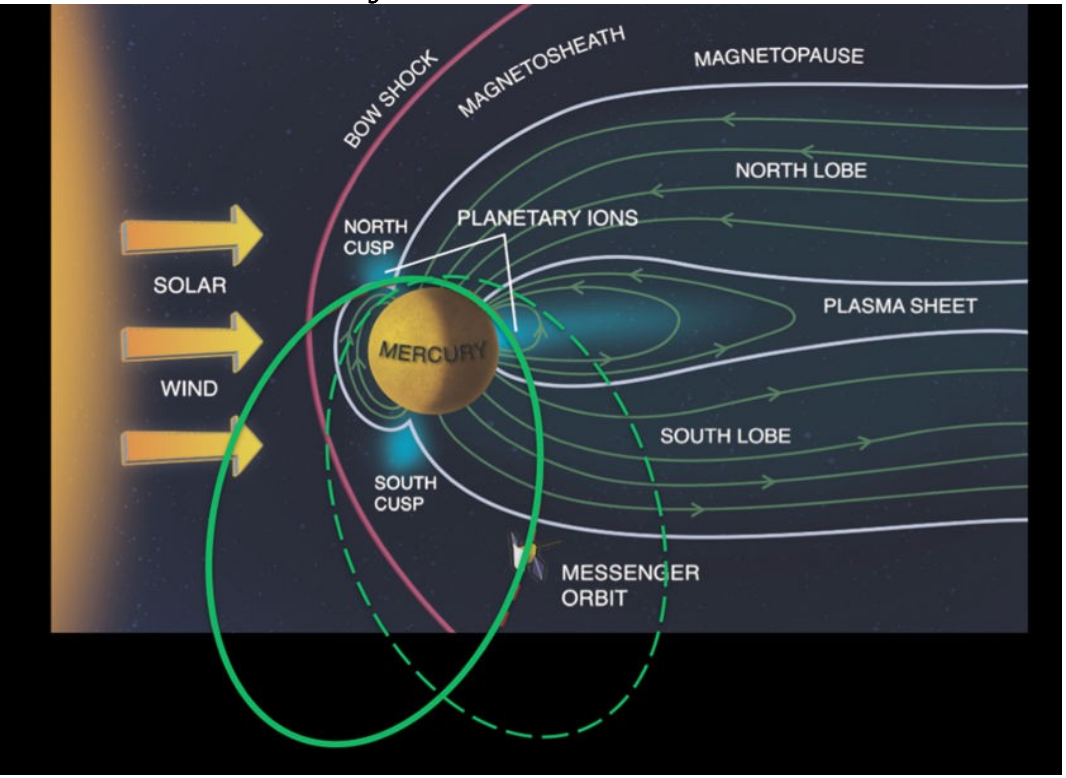

Mercury magnetic field is well measured thanks to Messenger probe. Its aurora is similar to Earth's.

Venus

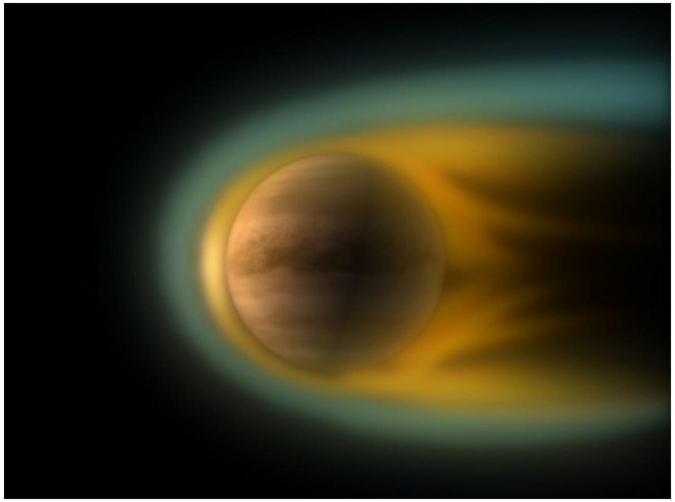

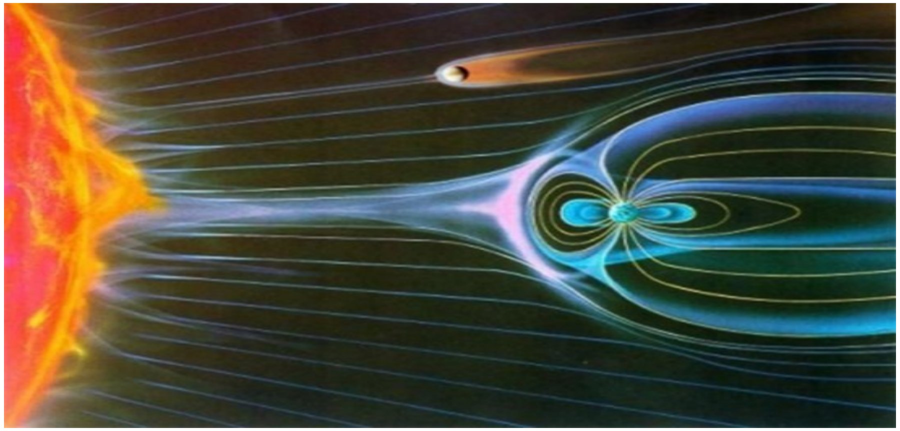

Venus has smaller aurora towards Sun than Earth, here I show a comparison.

Mars aurora

Even in the planets like Mars, which do not have significant magnetic field, we observe aurora, formed as a result of interaction of particles-here mostly protons- from the solar wind shock where the planet moves through the wind. It is most visible at the sunny side of the planet.

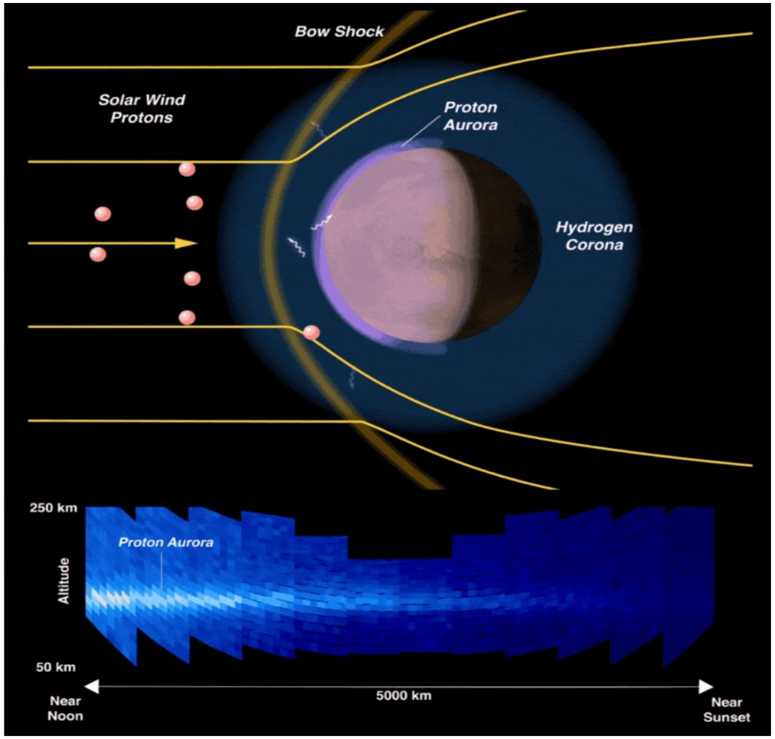

Auroras on large gaseous planets

Aurora is observed also on Jupiter and Saturn. On the gas planets aurora is visible mostly in ultra-violet, so we can observe it from outside our atmosphere.

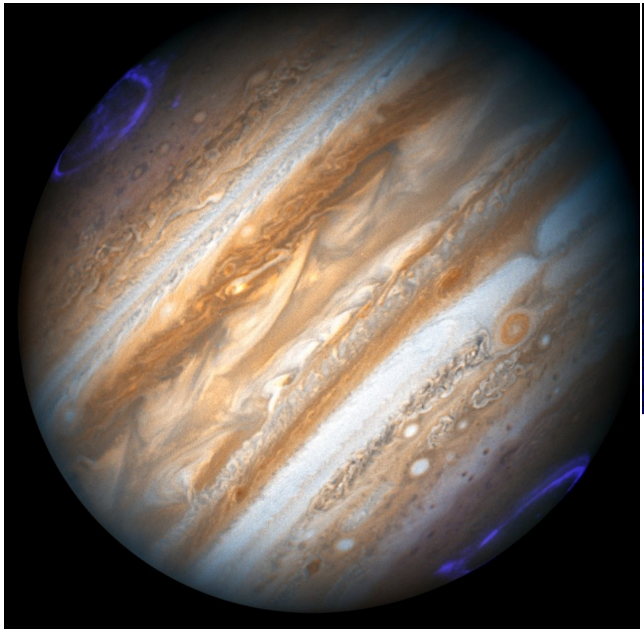

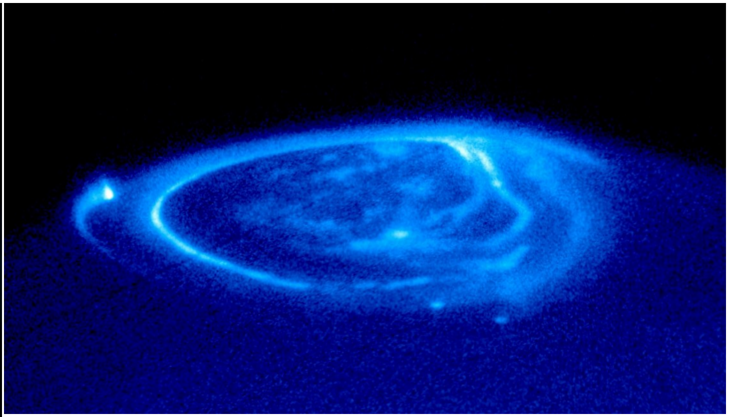

Spots in aurora on Jupiter are magnetically connected with its satellites: the spot on the left side is connected with Io, bottom two with Ganymede and Europe.

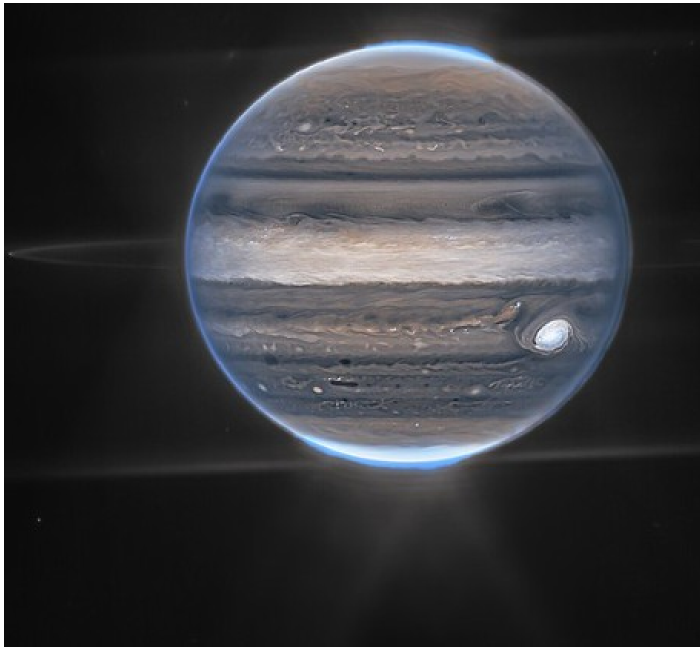

JWST’s capture of aurora on Jupiter

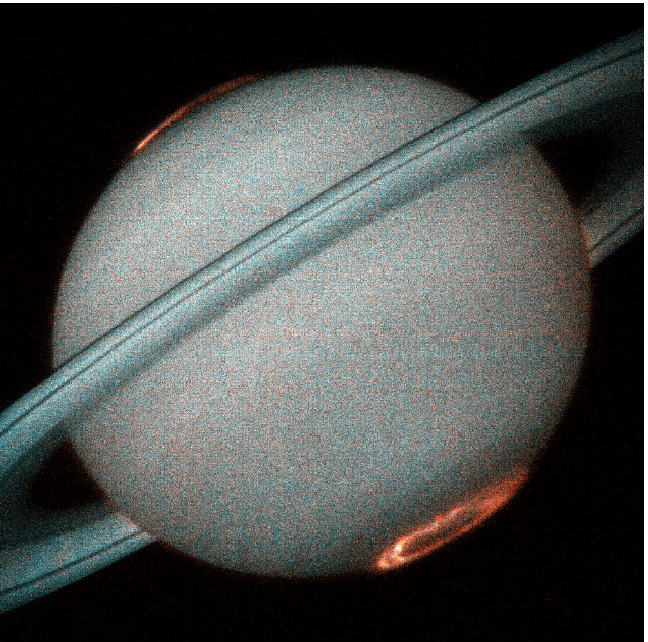

Saturn also features polar aurora:

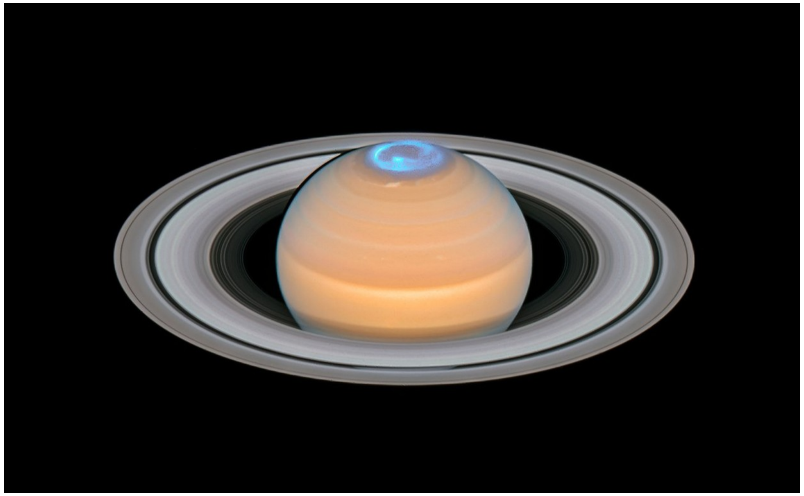

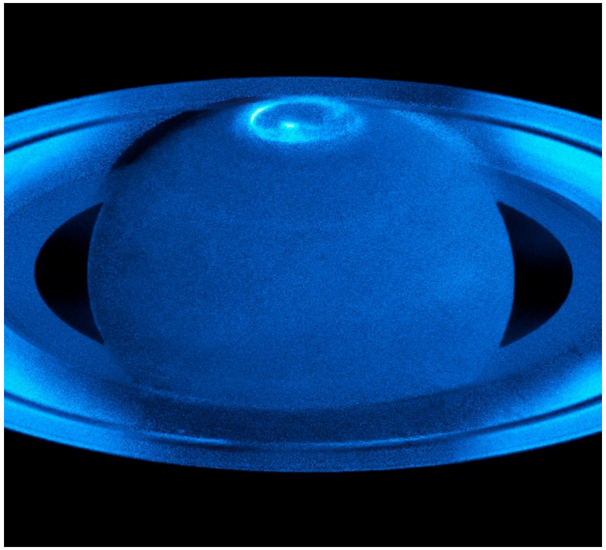

Aurora on Uranus

HST observed auroras on Uranus:

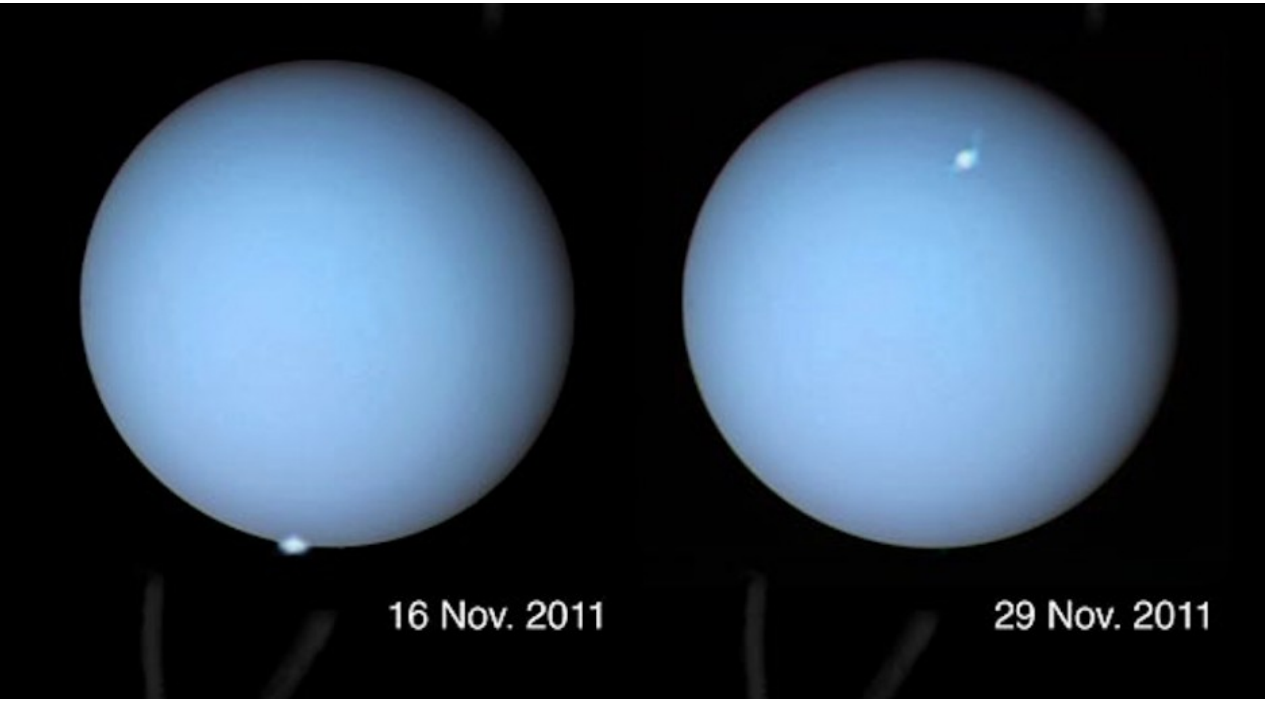

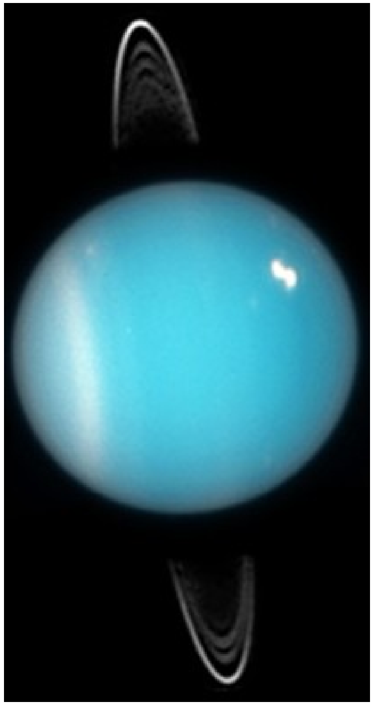

And Keck on Neptune:

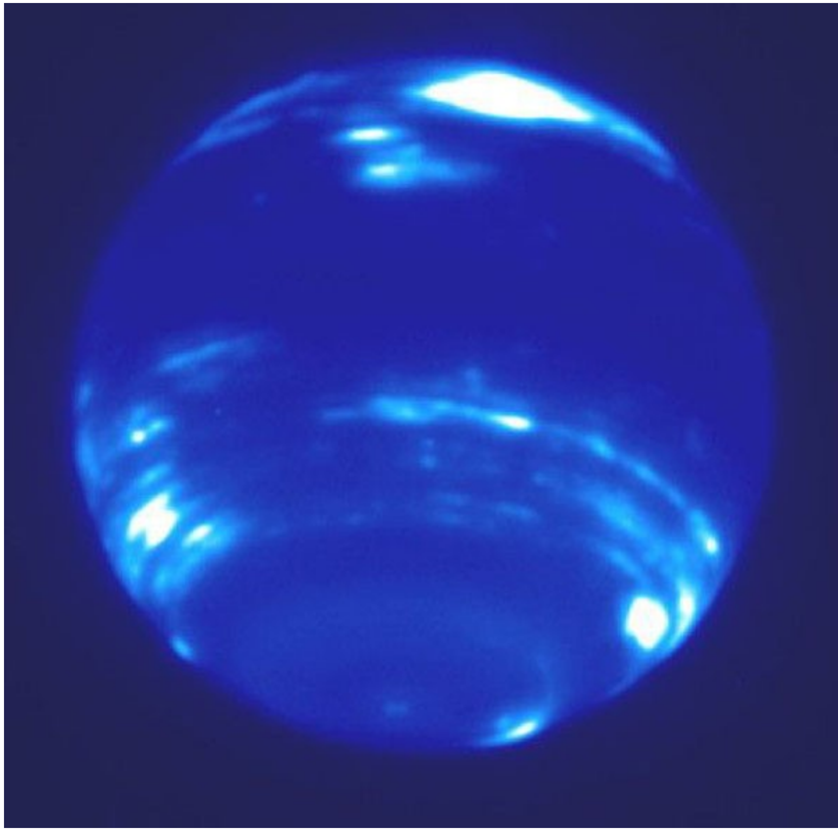

Extrasolar and exoplanet auroras

•As for now, we have an observation of extrasolar aurora on a brown dwarf LSR J1835+3259, 18 lyrs from us, in Lyra. There are more of similar objects which show characteristic spectral features which point to aurora. Shown is an artist impression, not the real observation. It is reddish aurora, from more hydrogen in the atmosphere, and about million times more intense, because of larger magnetic field.

•Such an aurora should also be of different nature, because there is no other star for producing the stellar wind.

•A model for aurora requires a continuously replenished body of plasma within the magnetosphere. This mass-loading can be achieved in multiple ways, including interaction with the interstellar medium, a volcanically active orbiting planet or magnetic reconnection at the photosphere. Alternatively, an orbiting planetary body embedded within the magnetosphere could provide magnetospheric interaction.

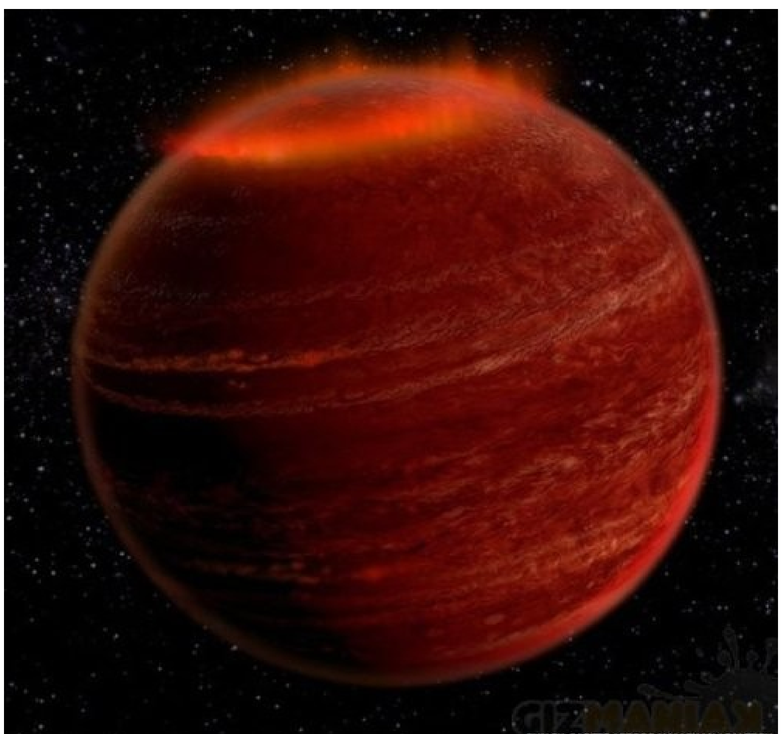

In the cases of **exoplanets**, we also expect auroras, and we can use the same simulations and make the predictions for different kinds of planets.

In the cases of **planets around pulsars**, which were actually the first observed exoplanets, we can expect similar effects. Because of much larger field involved, they could behave different from usual planet aurora.

Here we try to make the first such model, by introducing necessary modifications in our star-planet interaction setup.

Numerical simulations of star-planet interaction

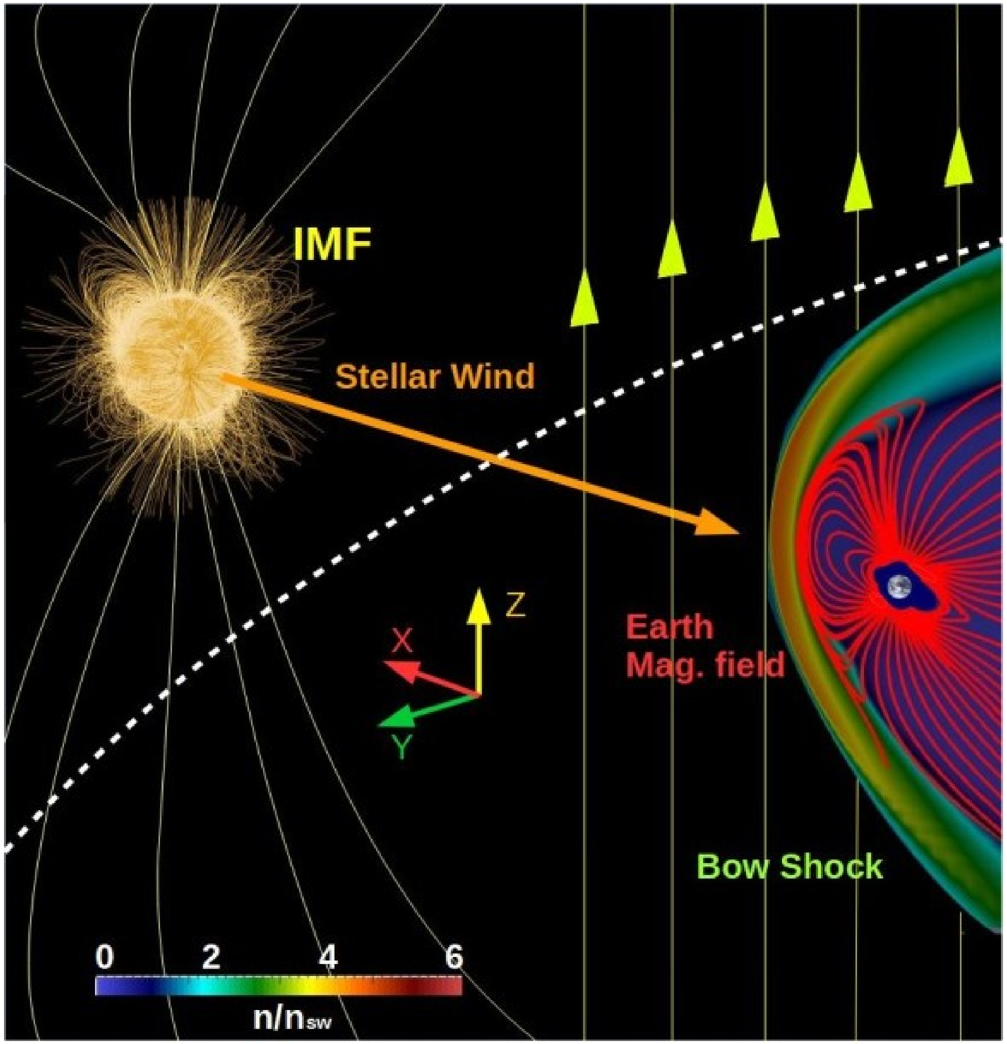

Fig. 1. 3D view of a typical simulation setup. We show the density distribution (color scale), Earth magnetic field lines (red lines), and IMF (yellow lines). The yellow arrows indicate the orientation of the IMF (northward orientation). The dashed white line shows the beginning of the simulation domain (the star is not included in the model).

- In a series of works by Varela et al. (e.g. A&A, 616, A182, 2018; A&A 659, A10, 2022) are given numerical simulations of planetary magnetospheric response in extreme solar wind conditions, using the PLUTO code.
- Such simulations are valid for Earth and exoplanets.
- We use this setup as a template for the much larger magnetic field of pulsar.

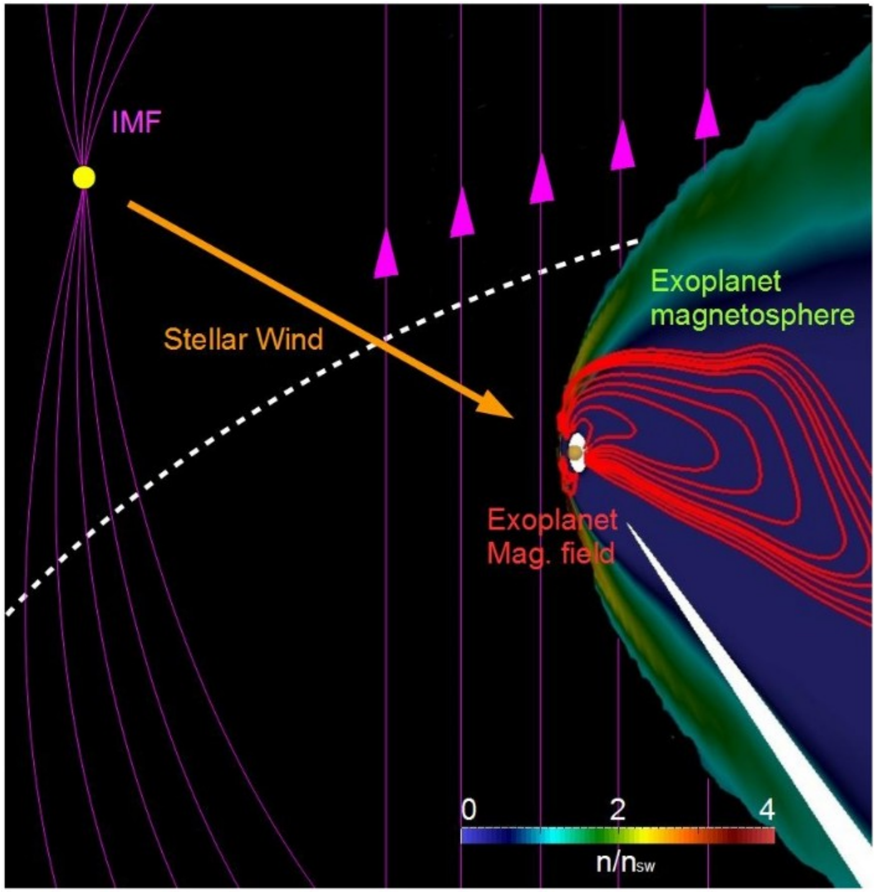

Fig. 1. 3D view of the system. Density distribution (color scale), field lines of the exoplanet magnetic field (red lines) and IMF (pink lines). The arrows indicate the orientation of the IMF (Northward orientation). Dashed white line shows the beginning of the simulation domain.

Numerical simulations of Sun-Earth magnetospheric interaction

Some results in the Sun-Earth simulations, where we can directly compare with measurements of the fields from orbiters.

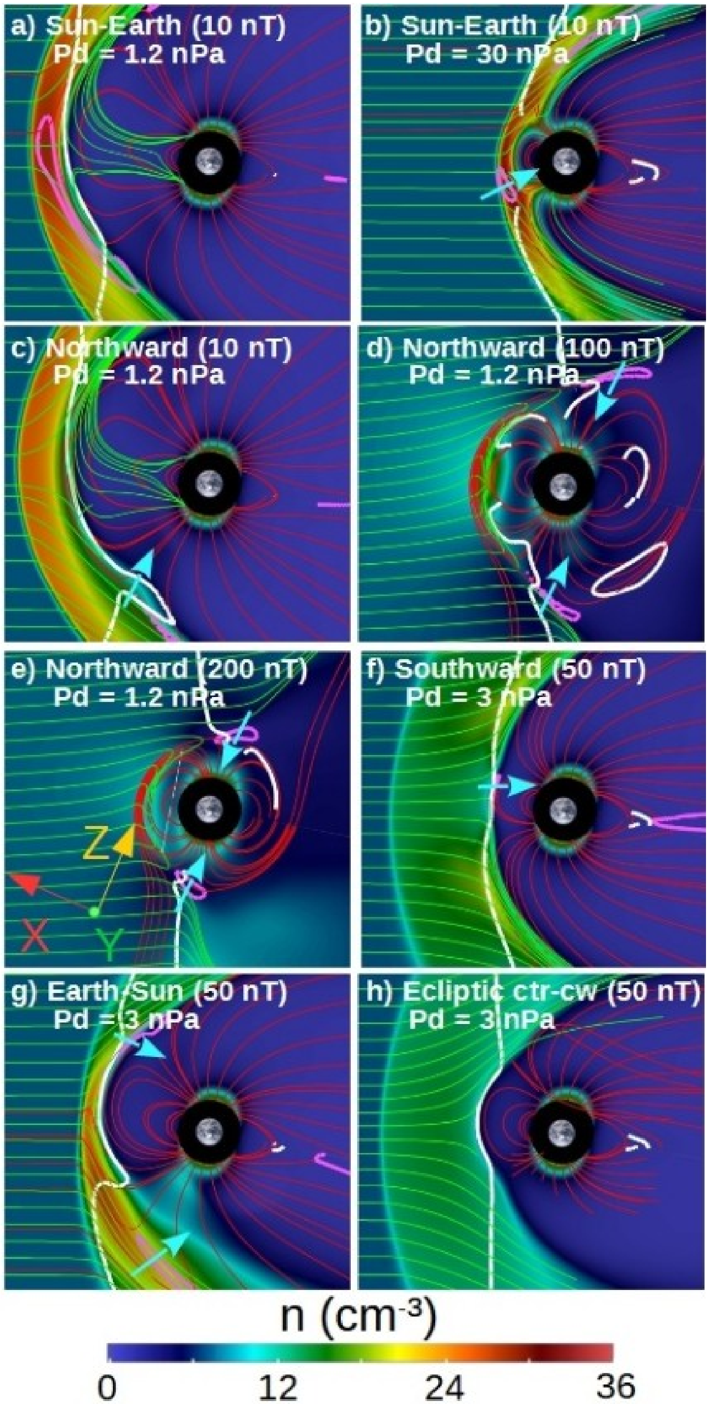

Fig. 2. Polar cut (XY plane) of the plasma density in simulations with (a) Sun–Earth IMF orientation $|B_{\mathrm{IMF}}| = 10\,\mathrm{nT}$ $P_{\mathrm{d}} = 1.2\,\mathrm{nPa}$, ($b$) Sun–Earth IMF orientation $|B_{\mathrm{IMF}}| = 10\,\mathrm{nT}$ $P_{\mathrm{d}} = 30\,\mathrm{nPa}$, ($c$) northward IMF orientation $|B_{\mathrm{IMF}}| = 10\,\mathrm{nT}$ $P_{\mathrm{d}} = 1.2\,\mathrm{nPa}$, ($d$) northward IMF orientation $|B_{\mathrm{IMF}}| = 100\,\mathrm{nT}$ $P_{\mathrm{d}} = 1.2\,\mathrm{nPa}$, ($e$) northward IMF orientation $|B_{\mathrm{IMF}}| = 200\,\mathrm{nT}$ $P_{\mathrm{d}} = 1.2\,\mathrm{nPa}$, ($f$) southward IMF orientation $|B_{\mathrm{IMF}}| = 50\,\mathrm{nT}$ $P_{\mathrm{d}} = 3\,\mathrm{nPa}$, ($g$) Earth–Sun IMF orientation $|B_{\mathrm{IMF}}| = 50\,\mathrm{nT}$ $P_{\mathrm{d}} = 3\,\mathrm{nPa}$, and ($h$) ecliptic ctr-cw IMF orientation $|B_{\mathrm{IMF}}| = 50\,\mathrm{nT}$ $P_{\mathrm{d}} = 3\,\mathrm{nPa}$. Earth magnetic field (red lines), SW stream functions (green lines), $|B| = 10\,\mathrm{nT}$ isocontour of the magnetic field (pink lines), and $v_{\mathrm{r}} = 0$ isocontours (white lines). The bold cyan arrows show the regions in which the plasma is injected into the inner magnetosphere.

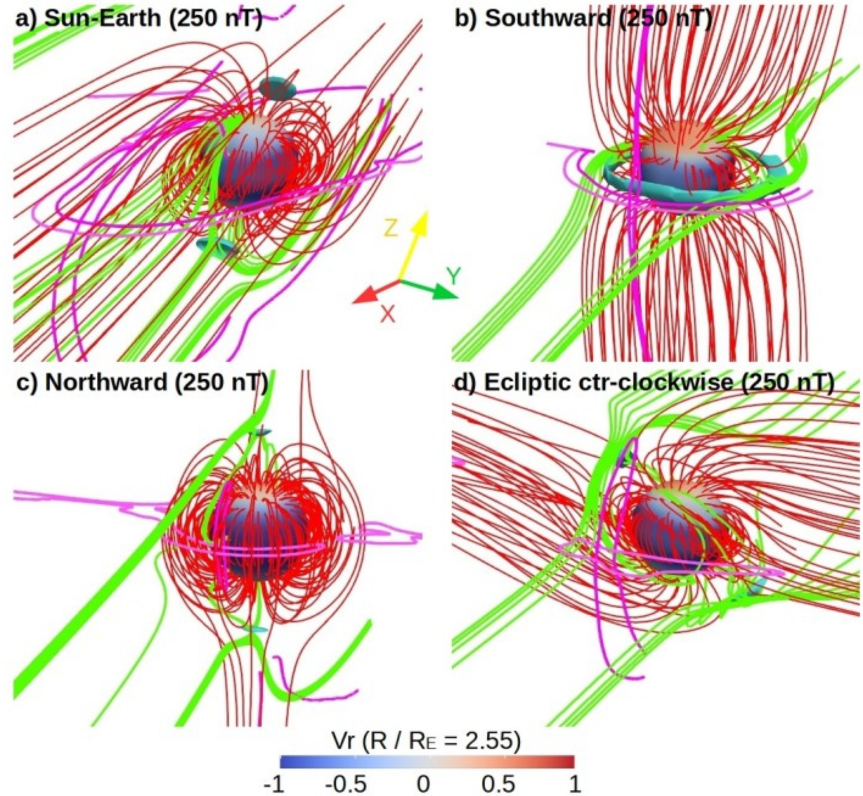

Fig. 3. 3D view of the Earth magnetosphere topology if $|B|_{\mathrm{IMF}} = 250\,\mathrm{nT}$ for (a) a Sun–Earth, (b) southward, (c) northward, and (d) ecliptic ctr-clockwise IMF orientations. We show the Earth magnetic field (red lines), SW stream functions (green lines), and isocontours of the plasma density for 6–9 cm^{-3}, indicating the location of the BS (pink lines). The cyan isocontours indicate the reconnection regions ($|B| = 60\,\mathrm{nT}$).

Numerical simulations of Sun-Mercury interaction

Similar study was also done for Mercury, where we have a wealth of data from Mariner 10 mission, which measured the dipole moment, and later Messenger mission, which provided more precise measurements for the multipolar representation.

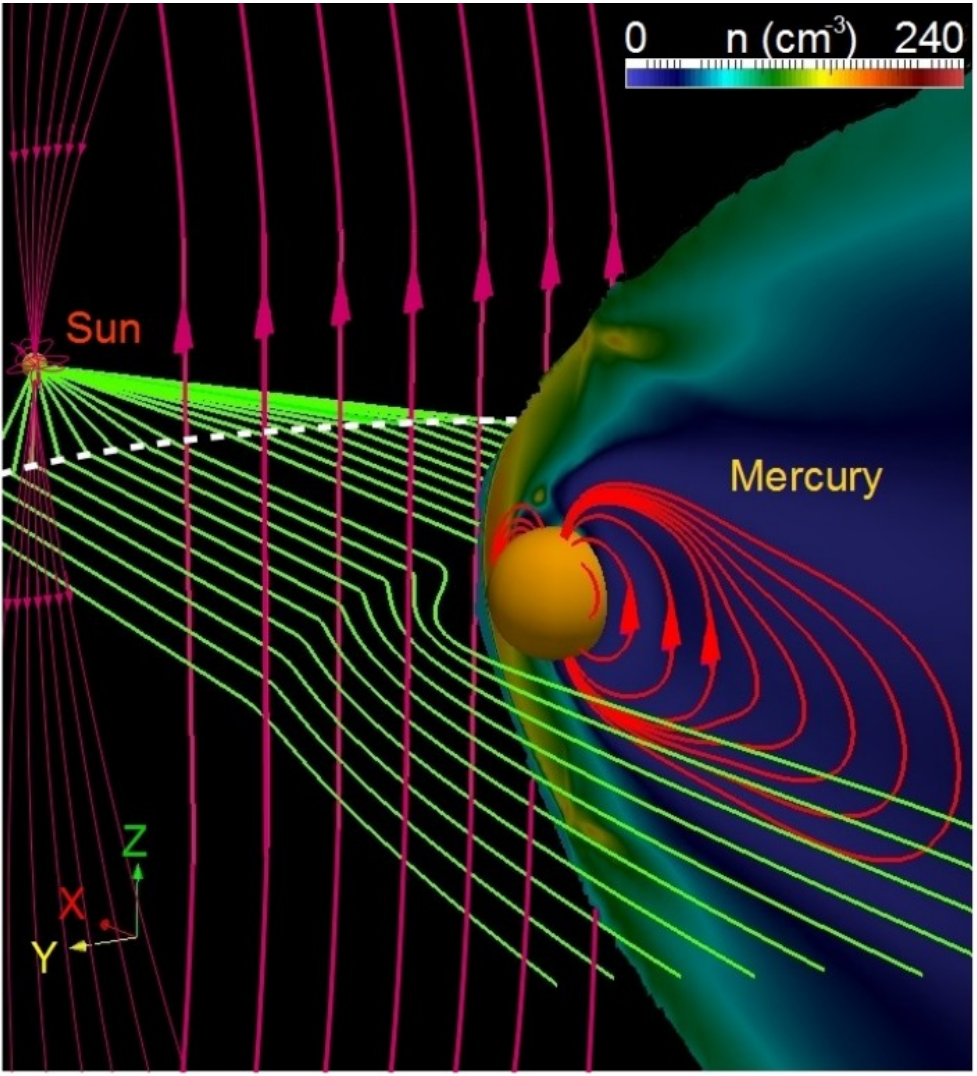

Fig. 1. 3D view of the system. Density distribution (color scale), field lines of the Hermean magnetic field (red lines), IMF (pink lines) and solar wind stream lines (green lines). The arrows indicate the orientation of the Hermean and interplanetary magnetic fields (case Bz). Dashed white line shows the beginning of the simulation domain.

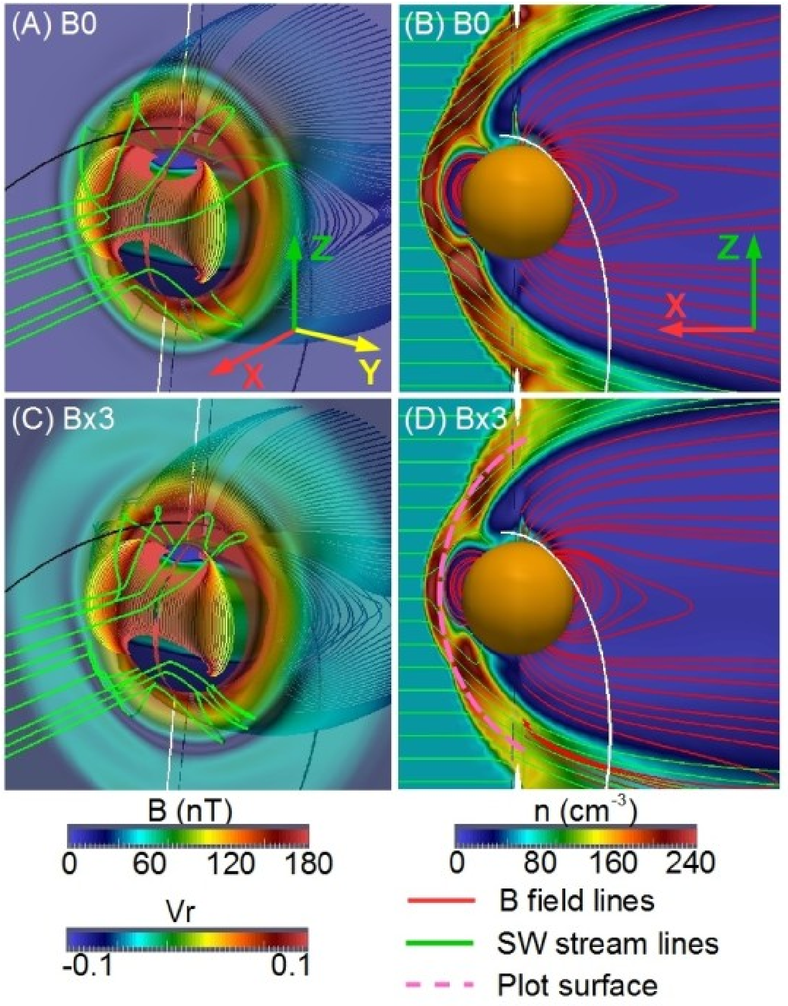

Fig. 2. Hermean magnetic field lines with the intensity imprinted on the field lines by a color scale for the reference case (A) and simulation Bx3 (C). Magnetic field intensity at the frontal plane $X = 0.3R_M$. SW stream lines (green). Inflow/outflow regions on the planet surface (blue/red). Polar plot of the density distribution (displaced $0.1R_M$ in Y direction) for the reference case (B) and simulation Bx3 (D). Dashed pink curve indicates the surface plotted in figures 3 and 4.

Planets around pulsars

•First exoplanets were found in orbit around a Galactic disk 6.2-ms pulsar PSR1257+12 (Wolszczan & Frail, 1992). PSR stands for “Pulsating Source of Radio” followed by the pulsar's right ascension and degrees of declination, B is added nowadays in the official name, to mark that coordinates are for the 1950.0 epoch, so official name is PSR B1257+12, or PSR J1300+1240 in epoch 2000, assigned with “J”. Usually pulsars older than 1993 retain this epoch names, but since the newer epoch includes position precisely to minutes in the name, all pulsars have their J epoch names.

•The precise timing of millisecond pulsars was instrumental for the discovery. This pulsar rotates about 161 times per second, 9650 rpm, period $P = 6.219 \times 10^{-3}$ s and a period derivative of $\dot{P} = 1.2 \times 10^{-19}$. In a standard magnetic dipole spindown model this gives a dipole magnetic field of $B = 3 \times 10^{19} (P\dot{P})^{1/2}$ G $\approx 8.8 \times 10^{8}$ G and a characteristic age $\tau = P/(2\dot{P}) = 8 \times 10^{8}$ yrs. It is the fastest moving pulsar, with transverse velocity 326km/s and its surface is hot, 29 000 K. It is 2300 ly (710 pc) from us, in the constellation Virgo.

•The detected planets (B and C today) were reported to have masses of at least 4.3 and 3.9 Earth masses. Their respective distances from the pulsar are 0.36 AU and 0.46 AU, and they move in almost circular orbits with periods of 66.6 and 98 days. The third planet of 0.02 Earth masses (=double Moon mass), which is a planet A today, with period of 25 days, positioned closer, at 0.19 AU, was identified after additional analysis of the data (Wolszczan 1994) [Scherer et al. (1997) pointed out that its 25.3 day orbital period is close to the solar rotation period at the 17deg solar latitude of PSR 1257+12, and suggested that the modulation might actually be due to modulation in the electron density of the solar wind in that direction. But, such an effect was not observed in other millisecond pulsars, and also the oscillation amplitude does not depend on the radio frequency (Wolszczan et al. 2000b), which would follow for a plasma effect. So, it is rather still a planet]. Orbits for A, B and C are similarly inclined 50, 53, 47 degrees, respectively. The fourth possible planet in this system (Wolszczan 1996) was later dismissed (Wolszczan et al. 2000a).

•In 2015, in NameExoWorlds campaign, pulsar, which is an undead star, got the name of a Lich, undead character from fantasy fiction, known for controlling other undead creatures with magic. Planets are named Draugr, Poltergeist and Phobetor for planets A, B and C, respectively (by increasing distance), by Norse mythology undead, noisy ghosts of supernatural world, and a character from Ovid's Metamorphoses (one of the thousand sons of Somnus=Sleep who appears in dreams in the form of beasts).

•This were the first exoplanets, which was long anticipated, but nobody expected it around a pulsar! The first planet around a “normal” star was found only in 1995. It was the first “hot Jupiter”, a large gaseous planet (named in NameExoWorlds as Dimidium=”half” in Latin, because of half Jupiter mass) with a surprising period of 4.2 days, orbiting very closely the star 51 Pegasi. This was awarded Nobel prize in 2019, because it was decades long search by Mayor & Queloz.

Formation of planets around pulsars

The formation mechanisms of planets around pulsars can be divided into presupernova and postsupernova scenarios.

-**Presupernova** scenario includes formation of planets around an ordinary star and either surviving the evolution (and a series of catastrophic events along it) or being captured by a NS.

• In **postsupernova** cases, planets are either formed from the material around newly formed NS (the **second generation planets**), or they are the last stage in the formation of some binary millisecond pulsars.

•For the rocky planets at circular orbits, a good possibility are mergers like WD+WD or WD+NS, or the remnant disk of the material from a Be star forming a binary with a NS. The first planets of Wolszczan best match the WD-WD merger scenario, so that planets are formed out of the debris of a merged companion star that used to orbit the pulsar when it was a white dwarf.

•Planets around pulsars seem to be rare, there are only few cases in about 3000 pulsars, all found by pulsar timing variations. Of more than 5000 currently known exoplanets, less than 10 around pulsars are confirmed

•A special feature because it *revived the field*: Interesting inconclusive one: (1982, 1994?) PSR B1937+21 close (few degrees) by the 1st discovered pulsar PSR B1919+21 (by Jocelyn Bell), this is the 1st discovered ms pulsar, 1.5ms (624 rotations in a second!), a companion of 0.001 M_Earth, like Ceres, at 2.7 AU, asteroid belt? More observations needed. Also points to a large precision of the method, when long observations available.

List of planets around pulsars

-(1993) PSR B1620−26 A + WD with one exoplanet (2.5+/- 1 M_Jupiter, orbiting them at 23 AU, period 36500 days~10 yrs, found from Doppler shifts it induced on the orbits of stars). It is in Scorpius, at a distance 12.4ly away, just outside the core of the globular cluster M4 which is 12.2 bln years old. Stars are hot: <30 000 K and <25 200 K. It is most probably a captured planet.

-(2006) 4U 0142+61, a magnetar (supernova about 100 000 yrs ago, 0.63 solar luminosities, rotates with 8.7s period) in Cassiopeia, at 13 000 ly from us, debris disk detected, at 1.6 mln km from the star, contains about 10 Earth masses of material, mostly heavier metals.

-(2011) The “diamond-planet” system PSR J1719–1438 is a millisecond pulsar surrounded by a Jupiter-mass companion ay least 23 times denser than water, thought to have formed via ablation (evaporation) of its donor star. It is a 27 000km radius 10^31 carats diamond crystal core remaining from the evaporated white dwarf, at 600 000 km from the star, has 2hr10’ rotation period. – of the similar kind is a Black Widow pulsar PSR B1957+20 (1988) in Sagitta constellation, with a period of 1.6ms and large mass, 1.6-2.4 M_Sun. It has a ~M_Jupiter companion, probably a brown dwarf, orbiting it with a period of 9.2hrs, making a 20min eclipses, through which the object was found.

-(1968 pulsar, 2013 asteroid?) PSR J0738−4042, encounter with an asteroid or in-falling debris from a disk. It is a bright, radio-emitting neutron star at a distance 37 000 ly in constellation Puppis, with rotational properties similar to the main population of middle aged, isolated, radio pulsars, P and Pdot 0.267 1/s (375ms) and -1/15e^-14 1/s^2, collected 24 yrs of data, so one can check the timing in detail.

-(1979, Demianski & Proszynski- planets rejected, 2017 still disputed) PSR B0329+54, 3 460 ly away in Camelopardalis, period 0.71452 s, 5 million yrs old. Remains the possibility of a long period planet.

-(1968 Puschino pulsar, 2014 planets) PSR B0943+10 is an 5mln years old pulsar in Leo, 2 000 ly away, with period 1.1s. Two gas giant planets,masses 2.8 and 2.6M_Jup with 730 and 1460 days orbital period, 1/8 and 2.9 AU radius orbits, respectively. There are more tentative objects with planets of Jupiter mass, like low luminosity (2017) PSR J2322−2650, with planet of 0.8M_Jup in the orbit with 0.32d at 0.01 AU; (2022) PSR J2007-3120 with a 0.008 M_J planet with 723d period; (2020, FAST) confirmed in globular cluster M13, PSR J1641+3627F, 3ms pulsar with a 0.16M_Sun mass companion, probably a WD, not a planet; the binary millisecond pulsar (2021, FAST) PSR J1641+3627E (also M13E) is a black widow with a companion mass around 19.42 M_J, 0.11d period; (2013) PSR J1544+493 eclipsing black widow 2.16 ms pulsar with a close companion of 18M_Jup at 2.19h orbit; (2016) PSR J0636+5129 with a 8M_J companion in 96min orbit; (1996, 2001?) PSR J2051−0827, 28.3M_Jup at 0.1d period orbit, (2000) PSR J1807-2459, 9.4M_J, 0.07days period.

Previous works on the topic

-Mottez & Heyvaerts (2011a,b) worked on planets around pulsars in the context of theory of electromagnetic interaction of stars and planets or small bodies. They extended the theory of Alfven wings to relativistic winds.

-In the Abstract of that A&A paper they wrote:" When the wind is relativistic but slower than the total Alfvén speed, a system of electric currents carried by a stationary Alfvénic structure is driven by the planet or by its surroundings. For an Earth-like planet around a "standard" second pulsar, the associated current can reach the same magnitude as the Goldreich-Julian current that powers the pulsar's magnetosphere." The energy which is released in the vicinity of the smaller body affects its orbit-for the objects of 100km diameter and below, the orbit could change significantly on the timescale of millions of years to 10 000 years, respectively.

-Most, if not all of the citations to the above papers came from the FRB community. There will probably be a larger following in the second generation planets formation framework, which is still building-up.

Numerical simulations: PLUTO MHD equations

Our work here emerged from a direct analogy: I was searching for a good learning topic for PLUTO simulations for CAMK summer students, apart from my usual thin accretion disc simulations. I remembered the work of Jacobo Varela with PLUTO, a collaboration started, and it was not a far shot from discussing millisecond pulsars with the Warsaw group to remembering that pulsars also have planets. Didactic result: Summer students in CAMK in 2022 and 2023 were learning PLUTO on star-planet magnetospheric interaction project. We worked in non-relativistic regime, using

6.2 The MHD Module

The MHD module is suitable for the solution of ideal or resistive (non-relativistic) magnetohydrodynamical equations. Source and definition files are located inside the Src/MHD directory.

With the MHD module, **PLUTO** solves the following system of conservation laws:

$$\begin{array}{lcll}
\dfrac{\partial \rho}{\partial t} & + & \nabla\cdot(\rho\boldsymbol{v}) & = 0 \\
\dfrac{\partial \boldsymbol{m}}{\partial t} & + & \nabla\cdot\left[\boldsymbol{m}\boldsymbol{v}-\boldsymbol{B}\boldsymbol{B}+\mathsf{I}\left(p+\dfrac{\boldsymbol{B}^2}{2}\right)\right]^T & = -\rho\nabla\Phi+\rho\boldsymbol{g} \\
\dfrac{\partial \boldsymbol{B}}{\partial t} & + & \nabla\times(c\boldsymbol{E}) & = 0 \\
\dfrac{\partial (E_t+\rho\Phi)}{\partial t} & + & \nabla\cdot\left[\left(\dfrac{\rho\boldsymbol{v}^2}{2}+\rho e+p+\rho\Phi\right)\boldsymbol{v}+c\boldsymbol{E}\times\boldsymbol{B}\right] & = \boldsymbol{m}\cdot\boldsymbol{g}
\end{array} \tag{6.4}$$

where ρ is the mass density, $\boldsymbol{m}=\rho\boldsymbol{v}$ is the momentum density, $\boldsymbol{v}$ is the velocity, p is the gas (thermal) pressure, $\boldsymbol{B}$ is the magnetic field[2] and E_t is the total energy density:

$$E_t=\rho e+\frac{\boldsymbol{m}^2}{2\rho}+\frac{\boldsymbol{B}^2}{2}\,. \tag{6.5}$$

where an additional equation of state provides the closure $\rho e=\rho e(p,\rho)$ (see Chapter 7). The source term on the right includes contributions from body forces and is written in terms of the (time-independent) gravitational potential Φ and and the acceleration vector $\boldsymbol{g}$ (see §5.4).

In the third of Eq. (6.4), $\boldsymbol{E}$ is the electric field defined by the expression

$$c\boldsymbol{E}=-\boldsymbol{v}\times\boldsymbol{B}+\frac{\eta}{c}\cdot\boldsymbol{J}+\frac{\boldsymbol{J}}{ne}\times\boldsymbol{B}\qquad\left(\boldsymbol{J}=c\nabla\times\boldsymbol{B}\right) \tag{6.6}$$

where the first term is the convective term, the second term is the resistive term (η denotes the resistivity tensor, see §8.2) while the third term is the Hall term (§8.1). Note that the speed of light c never enters

Numerical simulations of pulsar-planet interaction

In the pulsar planet case, we considered rocky planets, as in Wolszczan's system, and assumed that thy are not magnetized or are negligibly magnetized in comparison to the large magnetic field induced by the field carried in by the pulsar wind. Two simplest cases of the planetary surface are conductive and ferromagnetic.

Table 1. Parameters used in PLUTO setup file `pluto.ini` in our simulations for pulsar-planet setups with conductive and ferromagnetic planetary surfaces in comparison to Sun-Earth (CME) and Sun-Earth and Sun-Mercury (quiet) conditions. SW (Speed, MagField, Dens, and Temp) are setting the related initial values–in the Pulsar-planet case, SW corresponds to pulsar wind. PlanTemp sets the planetary temperature, and the Alfvén speed is limited by the AlfSpeedLimit. The radii R_{in} and $R_{sw,cut}$ set the inner boundary of the system and the radial position of the nose of the bow shock at the beginning of the simulation, respectively. The density floor is controlled by `dens_min`$=0.01\times$ `SWDens`.

Set-up	SWSpeed (cm s^{-1})	SWMagField (G)	SWDens (g cm^{-3})	SWTemp (K)	PlanTemp (K)	AlfSpeedLimit (cm s^{-1})	R_{in} (R_{NS})	$R_{sw,cut}$ (R_{NS})
Pulsar-planet	1.0×10^{9}	3	1.0×10^{-17}	2.0×10^{5}	1.0×10^{4}	1.0×10^{9}	1.0	1.0
Sun-Earth (CME)	1.0×10^{8}	1.0×10^{-3}	3.0×10^{-23}	1.0×10^{5}	1.0×10^{3}	5.0×10^{8}	3.0	6.0
Sun-Earth (quiet)	3.5×10^{7}	5.0×10^{-5}	6.0×10^{-24}	4.0×10^{4}	1.0×10^{3}	5.0×10^{8}	3.0	6.0
Sun-Mercury (quiet)	5.0×10^{7}	1.5×10^{-4}	2.0×10^{-23}	8.0×10^{4}	2.0×10^{3}	1.0×10^{8}	1.0	3.0

We increase the stellar magnetic field in the simulations-to accommodate for the large field we increase the density of the interplanetary medium, local magnetic field strength near the planet and stellar wind velocity. We probe for the different planetary surface boundary conditions (conducting or ferromagnetic) - this is potentially interesting for the planetary study: planets around NS could have some extreme physical properties, especially the second-generation planets, which could form around pulsars.

Numerical simulations – conducting planet

Conducting planet surface:

Bsw=3.0, Vsw=1.e9

Currents (yellow), Vsw(green), mag.field (red)

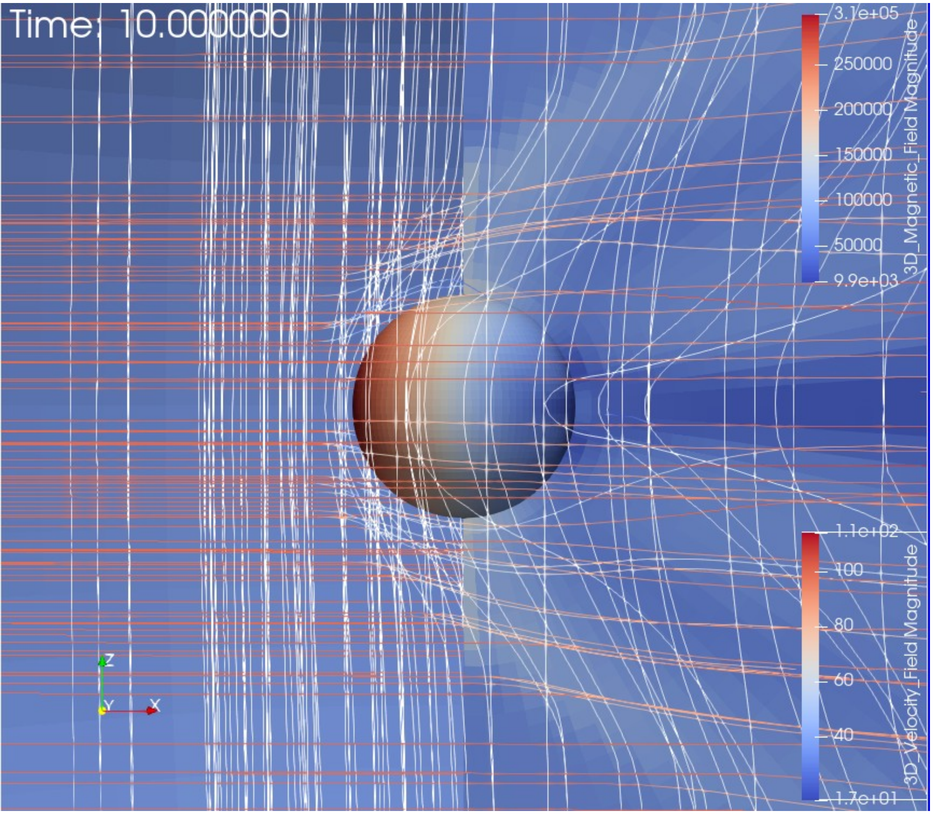

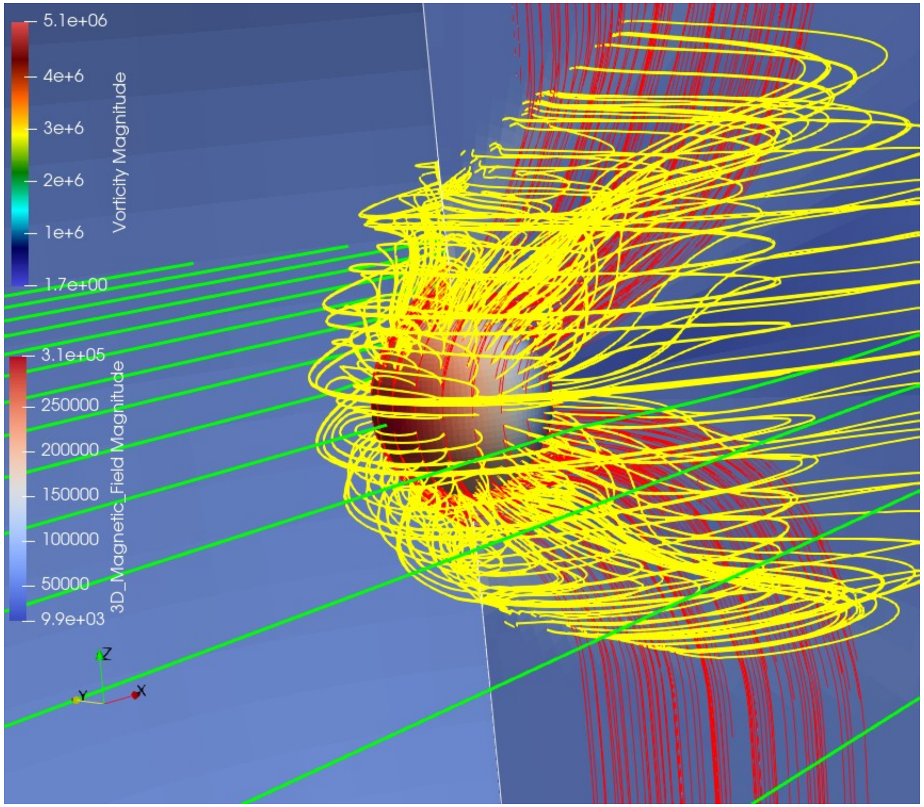

For the conducting planet atmosphere case, electric current loops remain close to the planet surface.

Numerical simulations – ferromagnetic planet

In the case of feromagnetic planet surface, results are different, currents point to an extended dipolar *electric field* structure. Work is in progress to understand the possible auroral effects.

Bsw=3.0, Vsw=1.e9

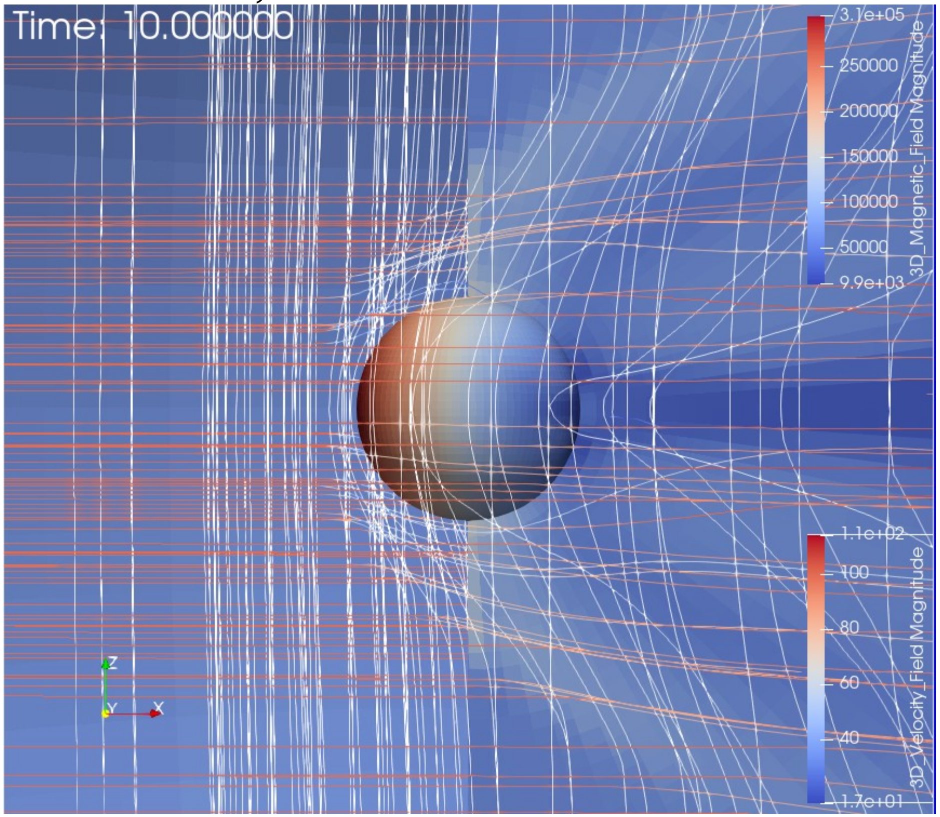

Currents (yellow), Vsw(green), mag.field (red)

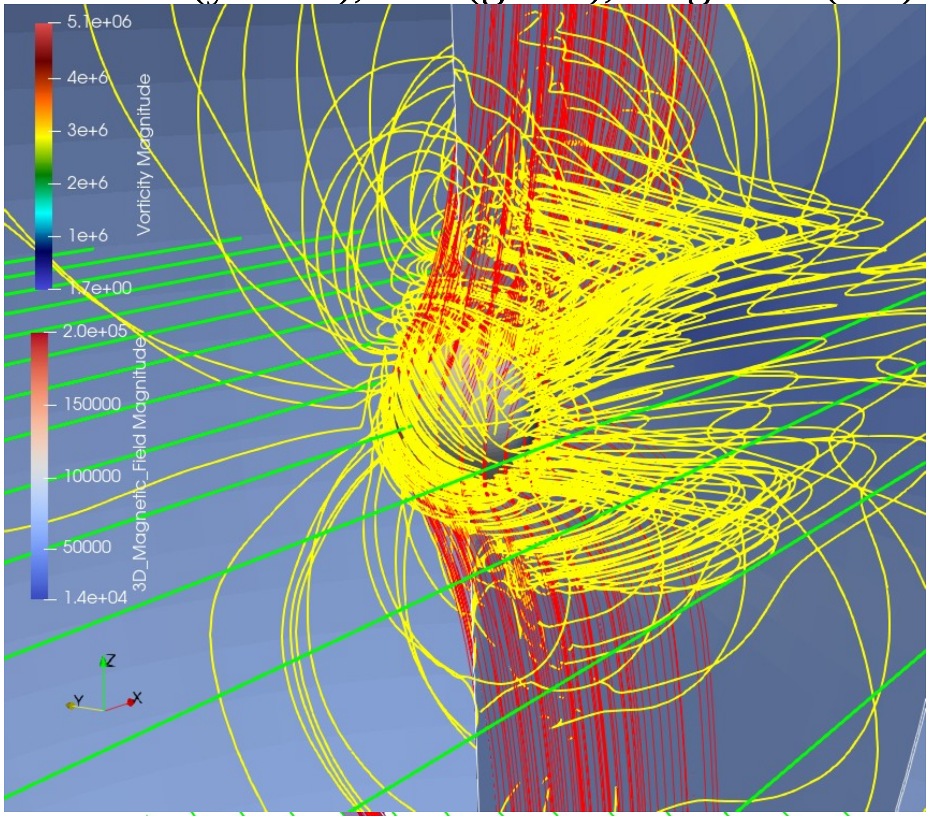

Equatorial view-Alfven “wings”:

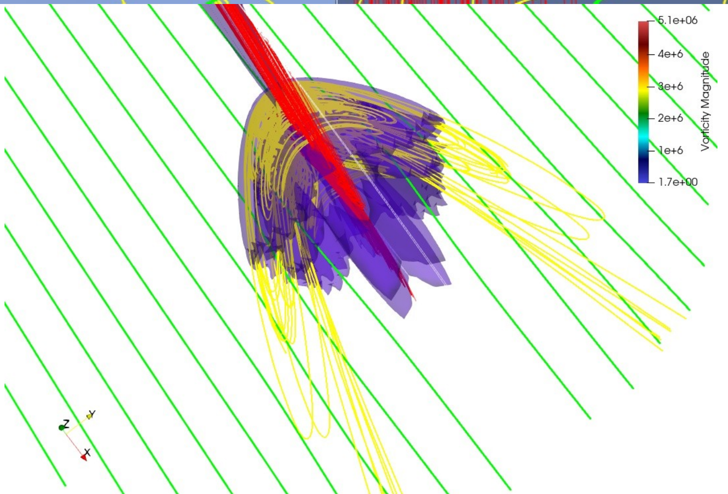

Radio emission patterns from non-magnetic planets

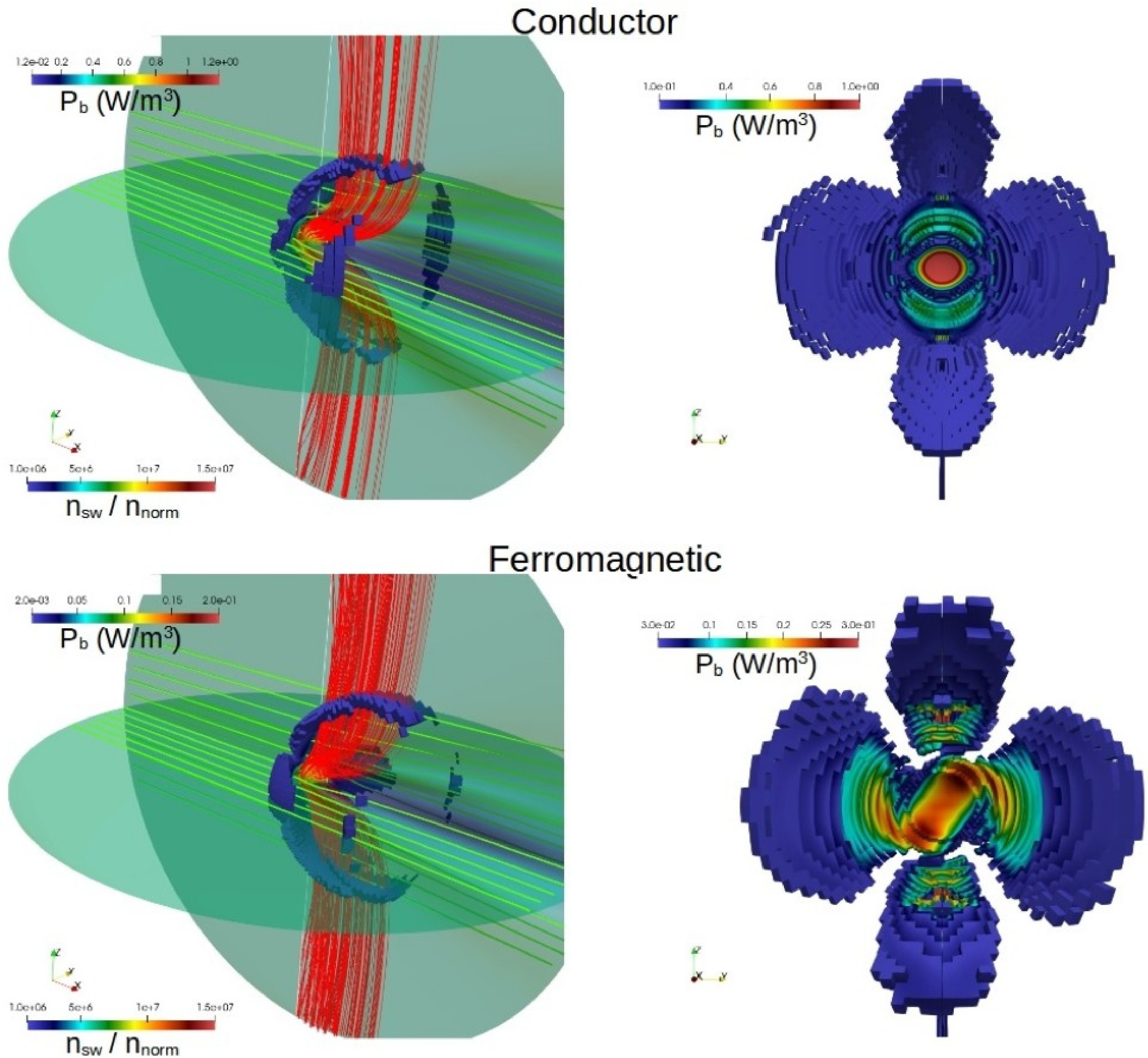

Left panels: Iso-volume of Poynting flux divergence in cases with non-magnetic planet. Red lines are the magnetic field lines and green lines are the velocity streamlines of stellar wind. *Right panels:* Mag. power in the same cases. A surface with the maximum radiated power is located in the nose of the bow shock, because of bending and compression of inter-planetary magnetic field.

- El.mag. emission is 100 million times more intense than in the Sun-Earth case.
- We suggest that it could be observable even with the current instruments.

Intensity of radio emission

LOFAR was able to detect low-frequency radio waves that were predicted from a M-type dwarf GJ 1151 (or a planet around it) which is located 25 light-years from Earth (Vedantham et al. 2020). This was, tentatively, the first signal detected from an extrasolar aurora.

What are the numbers for Wolszczan's pulsar? The only case of star-planet interaction without non-thermal radio emission arises when both the planet and stellar wind are non-magnetized. In all the other cases, even without intrinsic planetary magnetic field, there can arise intense radio emission. Based on the observations of magnetized planets in the Solar system, the empirical Radiometric Bode's law (RBL) is employed to estimate the intensity of radio emission, with the emission roughly proportional to the power from the stellar wind:

$$P_{rad} \propto P_{\text{in}} = P_{in,kin} + P_{\text{in},mag}, \tag{2}$$

with the kinetic power dissipation of the stellar wind protons hitting the magnetosphere of the planet $P_{in,kin}$ and the IMF Poynting flux on the planet's magnetosphere $P_{\text{in},mag}$:

$$P_{\text{in},kin} = m_{\text{p}} n v_{eff}^3 \pi R_{\text{m}}^2, \;\; P_{\text{in},mag} = \frac{B_\perp^2}{8\pi} v_{eff} \pi R_{\text{m}}^2. \tag{3}$$

The m_{p} is the proton mass, n the number density of the stellar wind around the planet, v_{eff} is the effective velocity of the stellar wind in the reference frame of the planet, R_{m} is the planetary magnetosphere radius, and $B_\perp$ is the IMF perpendicular to the stellar wind flow. The maximum emission frequency ν_{max} and characteristic plasma frequency ν_{min} are computed as:

$$\nu_{max} = \frac{eB_{\text{p},max}}{2\pi m_{\text{e}}} \sim 2.8 \text{ MHz} B_{\text{p},max}, \;\; \nu_{\text{min}} = \sqrt{\frac{ne^2}{\pi m_{\text{e}}}} \sim 8.98 \text{ kHz}\sqrt{n}, \tag{6}$$

where m_{e} and e are the electron mass and charge, and we measure $B_{\text{p},max}$ in Gauss and the plasma number density n in cm^{-3} (`SWDens` in Table 1). Emission is absorbed by the plasma below a lower limit of the frequency ν_{min}. In our

The radio power emitted from the star-planet interaction will depend on the type of interaction, and is given by scaling the $P_{in,kin}$ or $P_{\text{in},mag}$ by Jovian auroral radio emission. A statistical analysis of the results from simulations gives the expression for radio emission intensity, which depends on the strength of the magnetic field imposed on the planet by the incoming stellar wind B_{SW} and its dynamic pressure P_{d} (Zarka 2007, 2018; Varela et al. 2022):

$$P_{rad} \propto |B_{SW}|^{(0.9-1.22)} P_{\text{d}}^{(0.95-1.15)}. \tag{4}$$

The density of the radio flux from a planet at a distance d is then

$$\Phi = \frac{P_{rad}}{\Omega d^2 \Delta\nu}, \tag{5}$$

with $\Omega = 1.6$ sr being the solid angle of the beam of emitted radiation, which is set as equal to the value of Jovian emission (Zarka et al. 2004). The emission bandwidth $\Delta\nu$ is assumed to be the same as the maximum emission

Observational challenge

Most of the exoplanets we found until now are less than 2000 ly from us. Wolszczan's pulsar is about 750pc away, about 2100 ly from us, and there are many pulsars at about 250pc from us, among which some could have planets. We computed the radio emission from such planets, what is the amount of it reaching us, could we observe it?

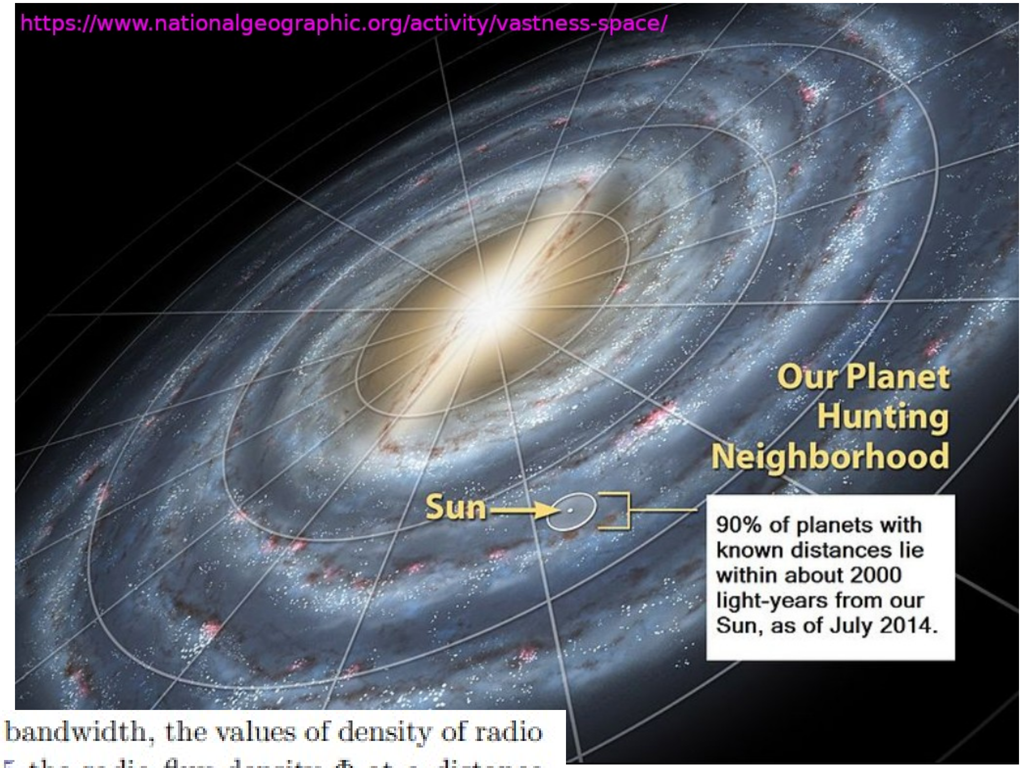

We computed the radio emission from such planets, what is the amount of it reaching us, could we observe it? LOFAR, MeerKAT, and the future SKA have minimal sensitivities of the order of 0.1, 0.01 and 0.001 mJy, respectively. Our preliminary results:

For the given integrated radio emission, distance of the planet and emission bandwidth, the values of density of radio flux for the pulsar-planet in the case with conductive planet, from the Eq. 5 the radio flux density Φ at a distance 700 pc, is given by

$$\Phi = \frac{1.9 \times 10^{18}}{1.6 \times (700 \times 3.1 \times 10^{16})^2 \times 5 \times 10^8} \times 10^{26} Jy = 0.5\ mJy, \quad (7)$$

and similarly, for the pulsar-planet in a ferromagnetic case $\Phi = 1.1$ mJy.

Set-up	$\Phi(700)$ (mJy)	$\Phi(250)$ (mJy)	P_{radio} (W)	$B_{p,max}$ (G)
Pulsar-planet (conductive)	0.5	4	1.9×10^{18}	3
Pulsar-planet (ferromagnetic)	1.1	9	4.3×10^{18}	3

PLUTO (Special) Relativistic MHD equations

For more than the initial study, we need to include the fact that the pulsar wind is relativistic, so we need to use the relativistic module of the PLUTO code:

6.4 The RMHD Module

The RMHD module implements the equations of (ideal) special relativistic magnetohydrodynamics in 1, 2 or 3 dimensions. Velocities are always assumed to be expressed in units of the speed of light. Source and definition files are located inside the Src/RMHD directory.

The RMHD module solves the following system of conservation laws:

$$\frac{\partial}{\partial t}\begin{pmatrix} D \\ \boldsymbol{m} \\ E_t \\ \boldsymbol{B} \end{pmatrix} + \nabla \cdot \begin{pmatrix} D\boldsymbol{v} \\ w_t\gamma^2\boldsymbol{v}\boldsymbol{v} - \boldsymbol{b}\boldsymbol{b} + \mathsf{I}p_t \\ \boldsymbol{m} \\ \boldsymbol{v}\boldsymbol{B} - \boldsymbol{B}\boldsymbol{v} \end{pmatrix}^T = \begin{pmatrix} 0 \\ \boldsymbol{f}_g \\ \boldsymbol{v}\cdot\boldsymbol{f}_g \\ \boldsymbol{0} \end{pmatrix} \tag{6.13}$$

where D is the laboratory density, $\boldsymbol{m}$ is the momentum density, E is the total energy (including contribution from the rest mass) while $\boldsymbol{f}_g$ is an acceleration term (see 6.3).

Primitive variables are similar to the RHD module but they also contain the magnetic field, $\boldsymbol{V} = (\rho, \boldsymbol{v}, p, \boldsymbol{B})$. The relation between $\boldsymbol{V}$ and $\boldsymbol{U}$ is

$$\begin{array}{rcl} D &=& \gamma\rho \\ \boldsymbol{m} &=& w_t\gamma^2\boldsymbol{v} - b^0\boldsymbol{b} \\ E_t &=& w_t\gamma^2 - b^0b^0 - p_t \end{array} \quad , \quad \left\{\begin{array}{rcl} b^0 &=& \gamma\boldsymbol{v}\cdot\boldsymbol{B} \\ \boldsymbol{b} &=& \boldsymbol{B}/\gamma + \gamma(\boldsymbol{v}\cdot\boldsymbol{B})\boldsymbol{v} \\ w_t &=& \rho h + \boldsymbol{B}^2/\gamma^2 + (\boldsymbol{v}\cdot\boldsymbol{B})^2 \\ p_t &=& p + \dfrac{\boldsymbol{B}^2/\gamma^2 + (\boldsymbol{v}\cdot\boldsymbol{B})^2}{2} \end{array}\right.$$

Results with the (Special) Relativistic PLUTO

While the numbers change, results appear similar. In the Solar case, the flow carried protons, and in the pulsar wind, the flow is electron-positron plasma. Now the fact if we have the sub- or super-Alfvenic flow becomes important. Both the v_A and pulsar wind are close to the speed of light, which defines the time scales in the simulations. We are still working on getting close to the expected values in the relativistic pulsar wind in our simulations.

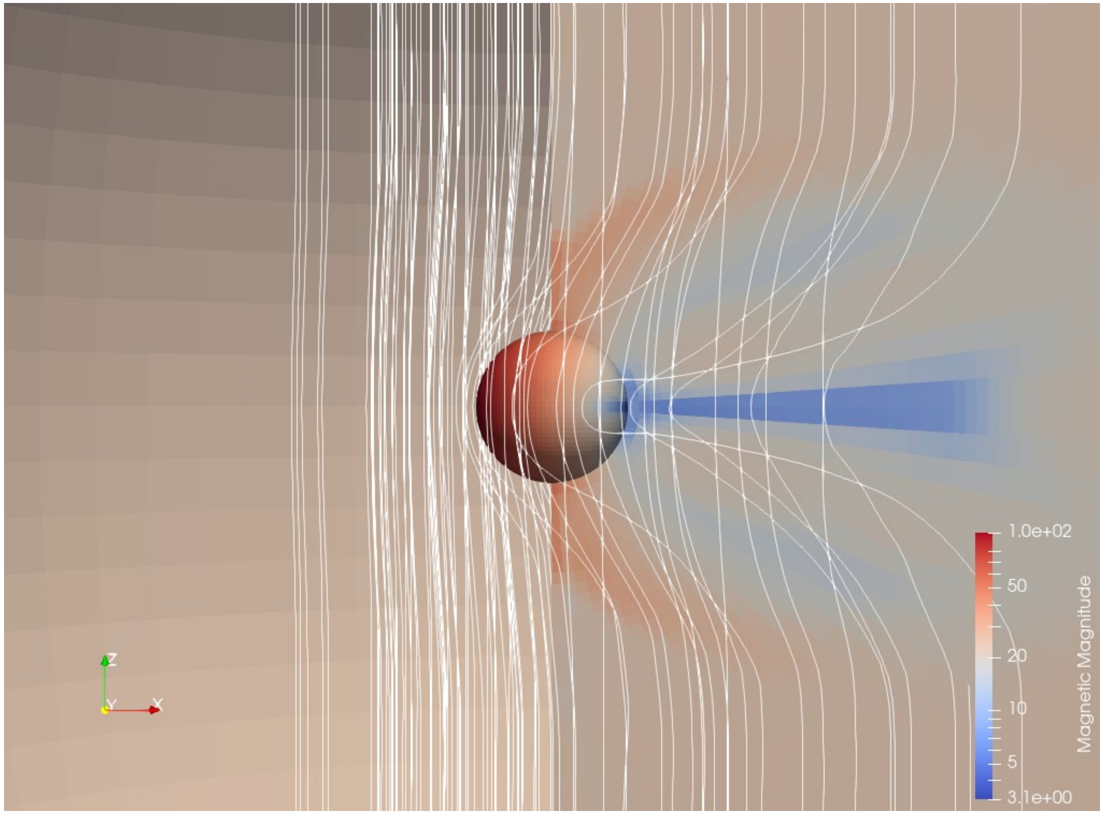

Summary

- Auroras are present in almost all planets in the Solar system.
- We have a tool to simulate the star-planet magnetospheric interaction.
- Planets around pulsars are not very often, <0.5%, with a variety of possible kinds of evolution. I give an overview for a better idea of current status.
- “Usual” rocky planets were the 1^{st} to be observed. Their evolution could be quite normal.
- We try our tool for aurora on the pulsar planets...plus relativistic module of PLUTO.
- Measuring the radio emission from pulsar planets would give us an additional window to study the pulsar wind.
- Radio emission from pulsar planets could be visible even with current instruments.